de Oliveira et al. Nanoscale Research Letters 2012, 7:607
http://www.nanoscalereslett.com/content/7/1/607

Nanoscale Research Letters
a SpringerOpen Journal

NANO EXPRESS Open Access

# Theoretical luminescence spectra in p-type superlattices based on InGaAsN

Thiago F de Oliveira[1], Sara CP Rodrigues[1*], Luísa MR Scolfaro[2], Guilherme M Sipahi[3] and Eronides F da Silva Jr[4]

**Abstract**

In this work, we present a theoretical photoluminescence (PL) for p-doped GaAs/InGaAsN nanostructures arrays. We apply a self-consistent $\vec{k}\cdot\vec{p}$ method in the framework of the effective mass theory. Solving a full $8\times8$ Kane's Hamiltonian, generalized to treat different materials in conjunction with the Poisson equation, we calculate the optical properties of these systems. The trends in the calculated PL spectra, due to many-body effects within the quasi-two-dimensional hole gas, are analyzed as a function of the acceptor doping concentration and the well width. Effects of temperature in the PL spectra are also investigated. This is the first attempt to show theoretical luminescence spectra for GaAs/InGaAsN nanostructures and can be used as a guide for the design of nanostructured devices such as optoelectronic devices, solar cells, and others.

**Keywords:** Dilute nitride semiconductor, Luminescence, $\vec{k}\cdot\vec{p}$ method, p-doped, Nanostructures

## Background

In the last decade, the study of quaternary InGaAsN alloy systems has attracted a great deal of attention due to its potential application in nanostructured devices such as next-generation multijunction solar cells and optoelectronic devices for optical communications [1-5]. Incorporation of a small amount of nitrogen (<2%) to InGaAs reduces the net strain because of the smaller atomic size of nitrogen (0.75 Å) compared with arsenic (1.33 Å), decreasing the bandgap due to a large bandgap bowing [6]. Therefore, by carefully controlling the composition ratios, one should be able to achieve InGaAsN epitaxial layers lattice-matched to GaAs substrates [7]. The use of these alloys in the manufacture of laser regions for optical communication emitting at the range of 1.3 to 1.5 μm shows several advantages, e.g., it has been demonstrated to be a low-cost replacement for directly modulated 1.3-μm InP devices used in network applications as wireless access points and Ethernet switches [8,9]. In addition, the diluted quaternary nitride alloys are of great interest for high-conversion efficiency solar cells and heterojunction bipolar transistors (HBT) with low turn-on voltage for portable devices [2-5]. For space photovoltaic applications, high-efficiency solar cell are advantageous for increasing the available electrical power or alternately reducing satellite mass and launch cost [2].

In order to improve the development of new dilute nitride-based devices, it is important to investigate the photoluminescence (PL) properties of semiconductor nanostructures [10]. Although an investigation on the PL properties of p-type-doped InGaAsN systems is of particular interest due to its potential usage in n-p-n HBT devices as the base layer [11-15], few reports are found on the literature. Generally, beryllium has been used as the p-type dopant in the InGaAsN layers [10,11]. From an experimental point of view, rapid thermal annealing (RTA) has been demonstrated to improve the PL intensity and the internal quantum efficiency of solar cells [6]. The real importance of this technique is that RTA can effectively reduce the composition fluctuation and suppress the InGaAs-rich phase [16]. This fact was also observed in GaAsN alloys, confirming the formation of localized states inside the wells [17].

In this work, we investigate the theoretical PL spectra calculations for p-doped GaAs/InGaAsN nanostructures. The calculations are performed within the $\vec{k}\cdot\vec{p}$ method by solving the full $8\times8$ Kane's Hamiltonian, generalized to treat different materials.

* Correspondence: srodrigues@df.ufrpe.br
[1]Departamento de Física, Universidade Federal Rural de Pernambuco, Rua Dom Manoel de Medeiro s/n, Recife, Pernambuco 52171-900, Brazil
Full list of author information is available at the end of the article

Strain effects due to the lattice mismatch between InGaAsN and GaAs are also taken into account. By varying the acceptor concentration and well width, we analyze the effect of exchange-correlation, which plays an important role in the potential profile and electronic transitions. We also investigate the effects of temperature in the PL spectra. These results can explain several important aspects on the optical properties of these nanostructured systems.

## Methods

The calculations are carried out by solving the $8 \times 8$ Kane's multiband effective mass equation (EME) which is represented with respect to a basis set of plane waves. We assume an infinite superlattice (SL) of squared well along the <001 > direction. The multiband EME is represented with respect to the plane waves with the wave vectors, $K = (2\pi/d)l$ ($l$ is an integer), equal to the reciprocal SL vectors. Rows and columns of the $8 \times 8$ Kane's Hamiltonian refer to the Bloch-type eigenfunctions $|jm_j \vec{k}\rangle$ of the $\Gamma_8$ heavy and light hole bands, $\Gamma_7$ spin-orbit hole bands, and $\Gamma_6$ electron bands; $\vec{k}$ denotes a vector of the first Brillouin zone.

Expanding the EME with respect to the plane waves $\langle z|K\rangle$ means representing this equation in terms of the Bloch function $\langle \vec{r}|jm_j \vec{k} + K\vec{e}_z\rangle$. For a Bloch function $\langle z|E\vec{k}\rangle$ of the SL corresponding to energy $E$ and the wave vector $\vec{k}$, the EME takes the following form [18,19]:

$$\begin{aligned}\sum_{j'm'_jK'} &\langle jm_j \vec{k}K|T + T_s + V_A + V_H + V_{HET} \\ &+ V_{XC}|j'm'_j \vec{k}K\rangle\langle j'm'_j \vec{k}K|\nu \vec{k}\rangle \\ &= E\left(\vec{k}\right)\langle jm_j \vec{k}K|\nu \vec{k}\rangle,\end{aligned} \tag{1}$$

where $T$ is the unperturbed kinetic energy term generalized for a heterostructure, $T_S$ is the strain energy term that originated from the lattice mismatch, $V_{HET}$ is the square potential due to the difference between energy gaps, $V_{XC}$ is the exchange-correlation potential, $V_H$ is the Hartree potential, and $V_A$ is the ionized acceptor potential [18-20]. The Luttinger parameters as well as the other terms appearing in the secular equation are to be taken for each epitaxial layer of the SL and were extracted from [18-21]:

$$\begin{aligned}\langle jm_jK|V_H + V_A|j'm'_jK'\rangle = &\frac{-4\pi e^2}{\varepsilon|K-K'|^2}\langle K|p(z) \\ &- N_A|K'\rangle\delta_{jj'}\delta_{m_jm'_j},\end{aligned} \tag{2}$$

with $N_A$ being the acceptor doping concentration and $p(z)$ the hole charge distribution which is given by the following:

$$p(z) = \sum_{jm_jk\in\text{empty}} |\langle zs|jm_j \vec{k}\rangle|^2. \tag{3}$$

The exchange-correlation potential contribution within LDA is taken into account as in our previous works; therefore, details can be found elsewhere [22,23].

From the calculated eigenstates, one can determine the luminescence spectra of the systems by applying the following general expression [24]:

$$\begin{aligned}I(\omega) = &\frac{2\hbar\omega^3}{c}\frac{e^2}{m_0c^2}\sum_k\sum_{n_e}\sum_{\substack{n_q \\ q=hh,lh,so}} f_{n_en_q}(k)N_{n_ek}\left[1-N_{n_qk}\right] \\ &\times\frac{1}{\pi}\frac{\gamma_{n_ek\ n_qk}}{\left[E_{n_e}(k)-E_{n_q}(k)-\hbar\omega\right]^2+\gamma^2_{n_ek\ n_qk}},\end{aligned} \tag{4}$$

where $e$ is the electron charge, $m_0$ is its mass, $\omega$ is the incident radiation frequency, $\gamma$ is the emission broadening, $n_e$ and $n_q$ are the electron and hole states associated to the transition, and $E_{n_e}$ and $E_{n_q}$ are the energies associated to them. $N_{n_ek}$ and $\left[1-N_{n_qk}\right]$ are the Fermi-like occupation functions for the states in conduction and valence bands, respectively. The oscillator strength, $f_{n_en_q}(k)$, is given by the following:

$$f_{n_en_q}(k) = \frac{2}{m_0}\sum_{\sigma_e\sigma_q}\frac{|\langle n_e\sigma_e k|p_x|n_q\sigma_q k\rangle|^2}{E_{n_e}(k)-E_{n_q}(k)}, \tag{5}$$

where $p_x$ is the dipole momentum in the direction $x$; $\sigma_e$ and $\sigma_q$ denote the spin values for electrons and holes, respectively. We consider the gap energy for InGaAsN alloys as described in [12]. We also used an approach for different temperatures, considering the Varshni correction as given in [25]. However, it is important to note that for the reported high concentrations of In (0.25 to 0.41) and N (0 to 0.052) at low temperatures ($T < 60$ K), the PL spectra shows an energy blueshift, mainly due to the recombination of excitons localized most likely in the In-N clusters [26].

## Results and discussion

Figure 1 shows the PL spectra at $T = 2$ K for p-type GaAs/$In_xGa_{1-x}As_{1-y}N_y$ SL with $x = 3\%$, $y = 1.3\%$, barrier width, $d_1 = 3$ nm, and well width, $d_2 = 3$ nm. From the literature [10,11,13], one can estimate the order of magnitude of hole concentrations, $N_A$. Four different hole concentrations, $N_A$, of this same order of were used, and they are $1 \times 10^{18}$, $2 \times 10^{18}$, $4 \times 10^{18}$, and $6 \times 10^{18}$ cm$^{-3}$. The systems

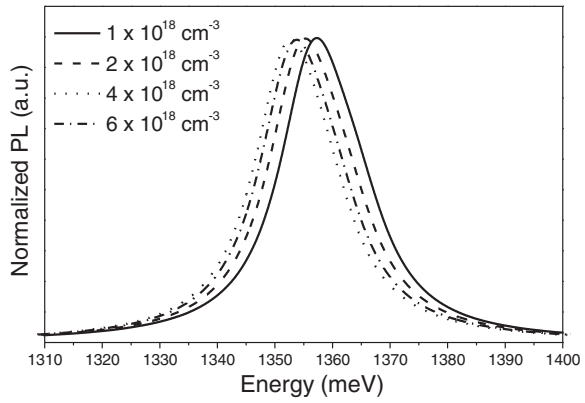


**Figure 1 Theoretical PL spectra, at 2 K, for unstrained p-doped $GaAs/In_xGa_{1-x}As_{1-y}N_y$ SL.** With $x = 3\%$, $y = 1.3\%$, barrier width, $d_1 = 3$ nm, and well width, $d_2 = 3$ nm. The acceptor concentration is varied for $N_A = 1 \times 10^{18}$ cm$^{-3}$ (solid line), $2 \times 10^{18}$ cm$^{-3}$ (dashed line), $4 \times 10^{18}$ cm$^{-3}$ (dotted line), and $6 \times 10^{18}$ cm$^{-3}$ (dot-dashed line).

present strain in the barrier as well as in the well though they are compensating each other. The peak in the spectra is assigned to the first electronic transition, from electron (E1)- to the heavy hole (HH1)-confined state. The notation indicates the first level occupied for each carrier. We observe a redshift in energy as the concentration increases, and after the value of $N_A = 4 \times 10^{18}$ cm$^{-3}$, we see a blueshift. This behavior is due to the different contributions for the Coulomb ($V_C$) and exchange-correlation potentials ($V_{XC}$) to the total potential, explained as follows. The competition between these potentials can generate a repulsive or attractive bending in the total potential since their sum will determine the shape of this bending inside the well. Thus, the energy levels lie near or far from the top of the valence band, decreasing or increasing the electronic transition. For a better comprehension, we present in Figure 2 the self-consistent heavy-hole (ground state) potential profiles inside the well for the same systems

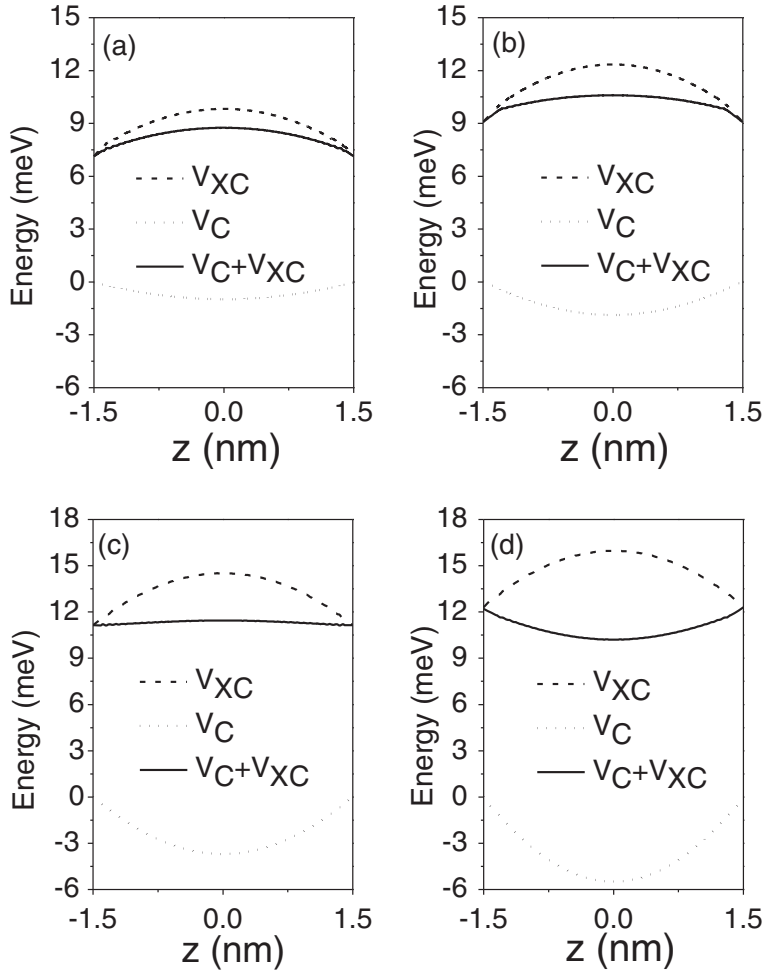


**Figure 2 Different contributions to the self-consistent heavy-hole potential for the same system of Figure 1.** With **(a)** $N_A = 1 \times 10^{18}$ cm$^{-3}$, **(b)** $N_A = 2 \times 10^{18}$ cm$^{-3}$, **(c)** $N_A = 4 \times 10^{18}$ cm$^{-3}$, and **(d)** $N_A = 6 \times 10^{18}$ cm$^{-3}$. Dotted line indicates the Coulomb potential, $V_C$; dashed line indicates the exchange-correlation potential, $V_{XC}$, and solid line indicates the total potential give by the sum of $V_C$ and $V_{XC}$.

described above. Clearly, it is possible to see that for $N_A = 1 \times 10^{18}$ cm$^{-3}$ and for $N_A = 2 \times 10^{18}$ cm$^{-3}$, $V_{XC}$ plays a major role in comparison with $V_C$, so the total potential has an attractive profile. This is a consequence of the charge-density localization, which is mostly concentrated at the well center. Therefore, since the exchange-correlation potential depends on the local charge density, it is expected that this one dominates over the Coulomb potential. For $N_A = 4 \times 10^{18}$ cm$^{-3}$, both potentials are practically the same, and the bending is almost flat. Above this concentration, the bending acquires a repulsive behavior. In this case, the Coulomb potential is more significant than the exchange-correlation potential.

In Figure 3, we analyze the PL spectra at $T = 2$ K by changing the well width, $d_2 = 2$, 3, 4, and 6 nm, for a fixed barrier $d_1 = 3$ nm for the same structures described above with $N_A = 2 \times 10^{18}$ cm$^{-3}$ and $N_A = 6 \times 10^{18}$ cm$^{-3}$. In both cases, we observe a redshift in energy as the well width increases. The character of the bending, repulsive or attractive, in the total potential profile remains unchanged in both cases; the levels are just closer to the top of the valence band as the well width increases, decreasing the optical transition.

The effects of temperature are analyzed in Figure 4, in which we show the calculated PL spectra as a function of temperature for the same system of Figure 3 with $d_1 = 3$ nm and $d_2 = 2$ nm and for $N_A = 6 \times 10^{18}$ cm$^{-3}$. There is a redshift in the position of the lowest peak of the spectra as the temperature increases. The first peak, as cited previously, corresponds to the first electronic transition, from electron (E1) to the heavy hole (HH1). The second peak is associated with the second transition, E1-LH1, with LH1 being the first light hole level. Actually, the first and second peaks are almost indistinguishable because the energy levels are very close. This fact occurs from $T = 2$ K up to $T = 200$ K. After that and for $T = 300$ K, we have the two lowest peaks, E1-HH1 and E1-LH1. Here, they are separated by a more significant amount of energy, followed by three more peaks, which correspond to E1-HH2, E1-HH3, and E1-SO1 (first split-off hole level), respectively. The latter shows a stronger peak due to a larger oscillator strength, which is larger than the superposition of the wave functions of the second, third, and fourth states

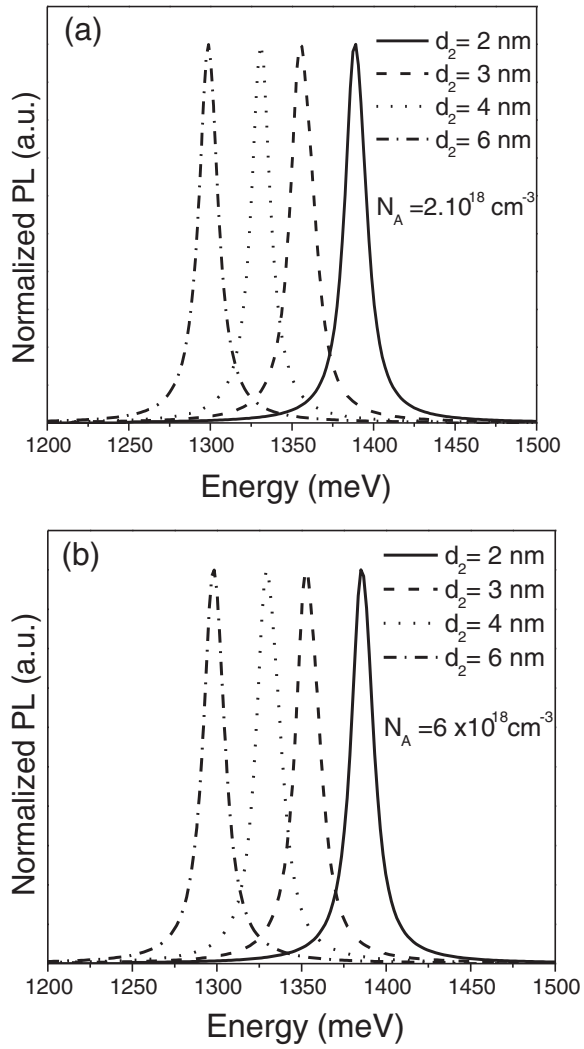


**Figure 3 Theoretical PL spectra at $T$ =2 K for the same system described in Figure 1.** With fixed $d_1 = 3$ nm for **(a)** $N_A = 2 \times 10^{18}$ cm$^{-3}$ and (**b**) $N_A = 6 \times 10^{18}$ cm$^{-3}$. The well width is varied for $d_2 = 2$ nm (solid line), 3 nm (dashed line), 4 nm (dotted line), and 6 nm (dot-dashed line).

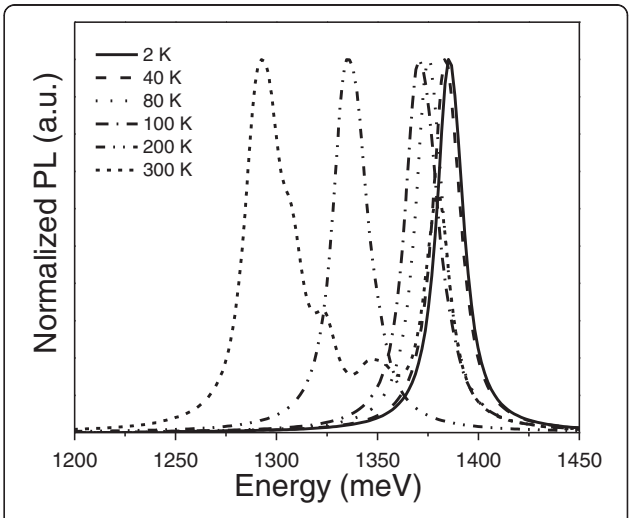


**Figure 4 Temperature dependence of the normalized calculated PL spectra as obtained in Figure 1.** With $d_1 = 3$ nm, $d_2 = 2$ nm, and $N_A = 6 \times 10^{18}$ cm$^{-3}$. From $T = 2$ K to $T = 200$ K, we have two peaks with close energies, which correspond to E1-HH1 and E1-LH1 electronic transitions. After that, for $T = 300$ K, there appear three more peaks, in addition to the first two lowest peaks, which are ascribed to the recombination involving the other excited hole states.

in the valence and conduction bands. As the temperature increases to 300 K, the main peak spans from transitions to the fundamental state to transitions to the first excited state and so on, giving rise to the multiple peaks seen. The redshift observed in the spectra is related to the InGaAsN gap shrinkage, according to the Varshni approximation [25].

## Conclusions

We present here for the first time the theoretical PL spectra for GaAs/InGaAsN systems obtained using self-consistent effective mass theory calculations. We noted a remarkable change in the total potential when the acceptor concentration increases. For the cases discussed here, changes in the well width do not change the shape of bending for the total potential. Furthermore, and as expected, we see a redshift in the PL spectra as the temperature increases. The present results show that in modulation p-doped GaAs/InGaAsN nanostructures, the many-body effects, such as exchange and correlation, must be taken into account for a realistic description of hole bands and potentials in these systems. These findings will certain have important implications for optical measurements, such as luminescence or absorption, towards developing new technologies based on nanostructured superlattices. This will be important in the development of new optoelectronic devices, solar cells, and other devices.

#### Competing interests

The authors declare that they have no competing interests.

#### Authors' contributions

TFO carried out the calculations. GMS, LMRS and EFSJ discussed the results and proposed new calculations and improvements. SCPR conceived the study and participated in its design and coordination. All authors read and approved the final manuscript.

#### Acknowledgements

The authors thank the support received from the Brazilian research financial agencies CNPq (grants no. 564.739/2010-3/NanoSemiCon, 302.550/2011-9/PQ, 470.998/2010-5/Univ, 472.312/2009-0/PQ, 303578/2007-6/PQ, and 577.219/2008-1/JP), CAPES, FACEPE (grant no. 0553–1.05/10/APQ), and FAPESP. Luísa MR Scolfaro also acknowledges partial support from the Materials Science, Engineering and Commercialization Program of Texas State University.

#### Author details

[1]Departamento de Física, Universidade Federal Rural de Pernambuco, Rua Dom Manoel de Medeiro s/n, Recife, Pernambuco 52171-900, Brazil. [2]Department of Physics, Texas State University, San Marcos, TX 78666, USA. [3]Instituto de Física de São Carlos, Universidade de São Paulo, CP369, São Carlos, São Paulo 13560-970, Brazil. [4]Departamento de Física, Universidade Federal de Pernambuco, Cidade Universitária, Pernambuco 50670-901, Brazil.

Received: 9 July 2012 Accepted: 19 October 2012
Published: 31 October 2012

#### References

1. Mair RA, Lin JY, Jiang HX, Jones ED, Allerman AA, Kurtz SR: **Time-resolved photoluminescence studies of $In_xGa_{1-x}As_{1-y}N_y$.** *Appl Phys Letters* 2000, **76:**188–190.
2. Kurtz SR, Allerman AA, Jones ED, Gee JM, Banas JJ, Hammons BE: **InGaAsN solar cells with 1.0 eV band gap, lattice matched to GaAs.** *Appl Phys Letters* 1999, **74:**729–731.
3. Milanova M, Vitanov P: **Dilute nitride GaAsN and InGaAsN layers grown by low-temperature liquid-phase epitaxy**. In *Solar Cells - New Aspects and Solutions*. Edited by Kosyachenko LA. Croatia: InTech; 2011:69–94.
4. Buyanova IA, Chen WM: *Physics and Application of Dilute Nitrides*. New York: Taylor & Francis; 2004 [Masnareh MO (Series Editor): *Optoelectronic Properties of Semiconductor and Superlattices*, vol 21].
5. Henini M: *Dilute Nitride Semiconductors*. Oxford: Elsevier; 2005.
6. Xin HP, Tu CW, Geva M: **Annealing behavior of p-type $Ga_{0.892}In_{0.108}N_xAs_{1-x}$ ($0 \le x \le 0.024$) grown by gas-source molecular beam epitaxy.** *Appl Phys Letters* 1999, **75:**1416–1418.
7. Hsu SH, Su YK, Chang SJ, Chen WC, Tsai HL: **InGaAsN metal–semiconductor-metal photodetectors with modulation-doped heterostructures.** *IEEE Photonic Tech Letters* 2006, **18:**547–549.
8. Ibáñez J, Alarcón-Lladó E, Cusco R, Artús L, Henini M, Hopkinson M: **Dilute (In, Ga)(As, N) thin films grown by molecular beam epitaxy on (100) and non-(100) GaAs substrates: a Raman-scattering study.** *J Mater Sci Mater Electron* 2009, **20:**S116–S119.
9. Liu W, Zhang DH, Fan WJ, Hou XY, Jiang ZM: **Intersubband transitions in InGaAsN/GaAs quantum wells.** *J Appl Phys* 2008, **104:**053119.
10. Xie SY, Yoon SF, Wang SZ: **Photoluminescence properties of *p*-type InGaAsN grown by RF plasma-assisted molecular beam epitaxy.** *Appl Phys A* 2005, **81:**987–990.
11. Xie SY, Yoon SF, Wang SZ, Sun ZZ, Chen P, Chua SJ: **Influence of Be on N composition in Be-doped InGaAsN grown by RF plasma-assisted molecular beam epitaxy.** *J of Crystal Growth* 2004, **260:**366–371.
12. Hoffmann A, Heitz R, Kaschner A, Lüttgert T, Born H, Egorov AY, Riechert H: **Localization effects in InGaAsN multi-quantum well structures.** *Mat Science and Engineering B* 2002, **93:**55–59.
13. Sun Y, Balkan N: **Energy and momentum relaxation dynamics of hot holes in modulation doped GaInNAs/GaAs quantum wells.** *J Appl Phys* 2009, **106:**073704.
14. Sun Y, Balkan N, Aslan M, Lisesivdin SB, Carrere H, Arikan MC, Marie X: **Electronic transport in n- and p-type modulation doped $Ga_xIn_{1-x}N_yAs_{1-y}$/GaAs quantum wells.** *J Phys Condens Matter* 2009, **21:**174210.
15. Khalil HM, Sun Y, Balkan N, Amann A, Sopanen M: **Nonlinear dynamics of non-equilibrium holes in *p*-type modulation-doped GaInNAs/GaAs quantum wells.** *Nanoscale Res Lett.* 2011, **6:**191–196.
16. Chen JF, Hsiao RS, Hsieh PC, Wang JS, Chi JY: **Effect of growth rate on the composition fluctuation of InGaAsN/GaAs single quantum wells.** *J Appl Phys* 2006, **99:**123718.
17. Buyanova IA, Chen WM, Monemar B: **Electronic properties of Ga(In)NAs alloys.** *MRS Internet J Nitride Semicond Res* 2001, **6:**1–19.
18. Rodrigues SCP, Sipahi GM, Scolfaro LMR, Leite JR: **Exchange-correlation effects on the hole miniband structure and confinement potential in zinc-blende $Al_xGa_{1-x}N$/GaN superlattices.** *J Phys Condens Matter* 2001, **13:**3381–3387.
19. Rodrigues SCP, Sipahi GM, Scolfaro LMR, Leite JR: **Hole charge localization and band structures of p-doped GaN/InGaN and GaAs/InGaAs semiconductor heterostructures.** *J Phys Condens Matter* 2002, **14:**5813–5827.
20. Rodrigues SCP, d'Eurydice MN, Sipahi GM, Scolfaro LMR, da Silva EF Jr: **White light emission from p-doped quaternary (AlInGa)N-based superlattices: theoretical calculations for the cubic phase.** *J Appl Phys* 2007, **101:**113706-1–113706-6.
21. Vurgaftman I, Meyer J, Ram-Mohan LR: **Band parameters for III–V compound semiconductors and their alloys.** *J Appl Phys* 2001, **89:**5815–5875.
22. Sipahi GM, Enderlein R, Scolfaro LMR, Leite JR: **Band structure of holes in p-type δ-doping quantum wells and superlattices.** *Phys. Rev. B* 1996, **53:**9930–9942.
23. Rosa AL, Scolfaro LMR, Enderlein R, Sipahi GM, Leite JR: **p-Type δ-doping quantum wells and superlattices in Si: self-consistent hole potentials and band structures.** *Phys. Rev. B* 1998, **58:**15675–15687.
24. Rodrigues SCP, Sipahi GM, Scolfaro LMR, Noriega OC, Leite JR, Frey T, As D, Schikora D, Lischka K: **Inter- and intraband transitions in cubic nitride quantum wells.** *phys stat sol (a)* 2002, **190:**121.

25. Mintairov AM, Kosel TH, Merz JL, Blagnov PA, Vlasov AS, Ustinov VM, Cook RE: **Near-field magnetophotoluminescence spectroscopy of composition fluctuations in InGaAsN.** *Phys Rev Letters* 2001, **87:**277401.
26. Polimeni A, Capizzi M, Geddo M: **Effect of nitrogen on the temperature dependence of the energy gap in $In_xGa_{1-x}As_{1-y}N_y$/GaAs single quantum wells.** *Phys Rev. B* 2001, **63:**195320.

doi:10.1186/1556-276X-7-607
**Cite this article as:** de Oliveira *et al.*: Theoretical luminescence spectra in p-type superlattices based on InGaAsN. *Nanoscale Research Letters* 2012 7:607.